A Porcine Wound Model of *Acinetobacter baumannii* Infection

Daniel V. Zurawski,[1,*,†] Chad C. Black,[2,*,†] Yonas A. Alamneh,[1] Lionel Biggemann,[1] Jaideep Banerjee,[1] Mitchell G. Thompson,[1] Matthew C. Wise,[3] Cary L. Honnold,[3] Robert K. Kim,[1] Chrysanthi Paranavitana,[1] Jonathan P. Shearer,[1] Stuart D. Tyner,[1] and Samandra T. Demons[1]

[1]*Wound Infections Department, Bacterial Diseases Branch, Walter Reed Army Institute of Research, Silver Spring, Maryland.*
[2]*Experimental Therapeutics Branch, Walter Reed Army Institute of Research, Silver Spring, Maryland.*
[3]*Veterinary Services Program, Department of Pathology, Walter Reed Army Institute of Research, Silver Spring, Maryland.*
[†]*These authors contributed equally to this study.*

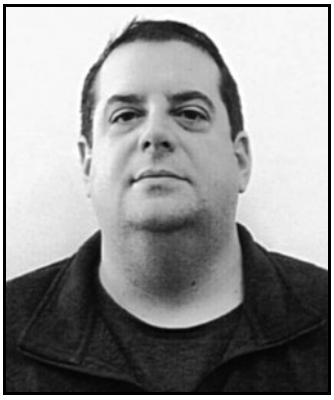

Daniel V. Zurawski, PhD

Submitted for publication February 21, 2018. Accepted in revised form June 24, 2018.

*Correspondence: Wound Infections Department, Bacterial Diseases Branch, Walter Reed Army Institute of Research, 2460 Linden Lane, Silver Spring, MD 20910
(e-mail: daniel.v.zurawski.civ@mail.mil).

Chad C. Black, DVM, PhD

*Correspondence: Experimental Therapeutics Branch, Walter Reed Army Institute of Research, 503 Robert Grant Avenue, Silver Spring, MD 20910
(e-mail: chad.c.black.mil@mail.mil).

Objective: To better understand *Acinetobacter baumannii* pathogenesis and to advance drug discovery against this pathogen, we developed a porcine, full-thickness, excisional, monospecies infection wound model.
Approach: The research was facilitated with AB5075, a previously characterized, extensively drug-resistant *A. baumannii* isolate. The model requires cyclophosphamide-induced neutropenia to establish a skin and soft tissue infection (SSTI) that persists beyond 7 days. Multiple, 12-mm-diameter full-thickness wounds were created in the skin overlying the cervical and thoracic dorsum. Wound beds were inoculated with 5.0×10^4 colony-forming units (CFU) and covered with dressing.
Results: *A. baumannii* was observed in the wound bed and on the dressing in what appeared to be biofilm. When bacterial burdens were measured, proliferation to at least 10^6 CFU/g ($\log_{10}6$) wound tissue was observed. Infection was further characterized by scanning electron microscopy (SEM) and peptide nucleic acid fluorescence *in situ* hybridization (PNA-FISH) staining. To validate as a treatment model, polymyxin B was applied topically to a subset of infected wounds every 2 days. Then, the treated and untreated wounds were compared using multiple quantitative and qualitative techniques to include gross pathology, CFU burden, histopathology, PNA-FISH, and SEM.
Innovation: This is the first study to use *A. baumannii* in a porcine model as the sole infectious agent.
Conclusion: The porcine model allows for an additional preclinical assessment of antibacterial candidates that show promise against *A. baumannii* in rodent models, further evaluating safety and efficacy, and serve as a large animal in preclinical assessment for the treatment of SSTI.

Keywords: *Acinetobacter baumannii*, ESKAPE pathogens, antibiotic testing, polymyxins, preclinical evaluation

INTRODUCTION

ACINETOBACTER BAUMANNII IS opportunistic gram-negative coccus capable of causing multidrug-resistant (MDR) infections. Over the last 10–15 years, the organism has been increasingly recovered from both civilian hospital patients and soldiers wounded in Iraq and Afghanistan,[1,2] and reports of severe wound infections and skin and soft tissue infection (SSTI) caused by this pathogen are also increasing in frequency.[3–5] In the military health care system, infections are further complicated by the increased morbidity and lengthy hospitalizations associated with wound infection and osteomyelitis, which can often lead to amputations of extremities infected with *A. baumannii*.[6,7] In the civilian sector, *A. baumannii* infections can come in many varieties to include urinary tract, SSTI, diabetic wounds, ventilator-associated pneumonia, and necrotizing fasciitis.[8] A lack of antibiotic options further complicate the treatment of these infections. Over time, *A. baumannii* has become increasingly resistant to a broad range of antibiotics.[8,9] Specifically, *A. baumannii* strains have acquired resistance to most if not all aminoglycosides, carbapenems, cephalosporins, and tetracyclines, and many are considered extensively drug-resistant (XDR). Recently, even some colistin-resistant strains have emerged that are considered pandrug-resistant, which presents an even more daunting challenge for clinicians.[10–13]

To date, assessments of *A. baumannii* virulence have largely been conducted in *Galleria mellonella* or with murine and rat pulmonary models of infection.[14,15] Given their cost, availability, and ease of husbandry, these models provide an inexpensive tool by which baseline data can be attained. However, insect and rodent models are not necessarily the most ideal model for the study of host–pathogen interactions especially with regard to wound infection and SSTI in humans. For example, when comparing to rodents, there is an increased amount of hair on their skin; this extra hair, when coupled with thinner dermal and epidermal layers of skin, can result in a limited histological interpretation of healing and wound pathology. Rodents also lack a layer of fat cells underneath the dermis, which is found in humans. Furthermore, rodents are generally recognized to heal through a combination of contraction and re-epithelialization.[16] In contrast, humans heal by re-epithelialization only.[16] Despite these limitations, we were still able to develop mouse models of wound infection for both *A. baumannii*[17] and *Klebsiella pneumoniae*.[18] These models have allowed for the initial *in vivo* exploration of clinically used antibiotics as well as the ability to compare them to novel antibacterial therapies in something resembling an SSTI indication.[17–19] While these models provide a first valuable step for antibacterial evaluation, a larger animal with skin similar to humans is more ideal. Therefore, a complimentary approach to the rodent SSTI models would be a porcine model of wound infection. From an anatomical and physiological standpoint, porcine skin bears similarities to humans in terms of thickness, cellularity, elasticity, healing times, and hair follicle distribution. Histologically, vessel size and orientation are also similar, further supporting the thought that a porcine model would be ideal in wound healing studies.[20,21] Some groups have exploited the use of porcine tissue to evaluate *ex vivo* infections.[22,23] However, these systems, while relevant, lack the systemic immune response to the infection. At present, porcine models of *A. baumannii* infection have been limited to burn models and polymicrobial infection[24] or diabetic hosts.[25]

While wound infection is considered polymicrobial, the contribution of *A. baumannii* is increasingly being tied to bad outcomes[26] and may need to be specifically treated. To develop better therapeutic options, several companies are working on small-molecule antibiotics that have a more narrow-spectrum activity with a focus on *Acinetobacter* species[8] and potentially could be topically applied. However, evaluation of novel *A. baumannii*-specific antimicrobials could be limited due to lack of a well-established mono-, rather than a polymicrobial, SSTI model.

In this work, we present an excisional, monospecies-infected porcine wound model, in which a diminutive inoculum of a clinically relevant XDR *A. baumannii* isolate can proliferate, develop infection, possibly form biofilms, and be effectively treated with antibiotics. This model can therefore simulate SSTI, allowing the researchers to garner greater insight into the nature of *A. baumannii* pathogenicity in a host that better resembles a patient and can be used to assess novel antimicrobial compounds as future treatments.

CLINICAL PROBLEM ADDRESSED

SSTI are responsible for about 14 million outpatient visits and over 850,000 hospital visits per year in the United States. In 2013, the Food and Drug Administration defined a class of SSTI as acute bacterial skin and skin structure infections (ABSSSI) and provided guidance for companies looking to develop new drugs for this indication. As new analogues of antibiotics, novel compounds, and nontraditional approaches enter the drug

pipeline to address ABSSSI, many forms of testing are required before they enter clinical trials. Bacterial infections are the main cause of ABSSSI and SSTI, and in particular, the ESKAPE (*Enterococcus faecium*, *Staphylococcus aureus*, *K. pneumoniae*, *A. baumannii*, *Pseudomonas aeruginosa*, and *Enterobacter* species) pathogens are the dominant species that are both drug-resistant and require new treatments. Animal models for SSTI and ABSSSI using these bacterial species are desired as researchers evaluate their new treatments before human trials are considered.

MATERIALS AND METHODS

Bacterial strain and inoculum preparation

A. baumannii clinical isolate AB5075 was used in all experiments. This strain was isolated from a patient at the Walter Reed Army Medical Center between 2008 and 2009, has been extensively characterized, and used in previous mouse models of lung and wound infection by our research group.[14,17,27] AB5075 is XDR but susceptible to polymyxin B (susceptible at 0.5 μg/mL determined by *E*-test). Bacteria were cultured in Lennox Luria–Bertani (LB) media (Becton, Dickinson and Co., Sparks, MD). One hundred microliters of AB5075 overnight culture was subcultured into 10 mL of LB and then grown at 37°C and shaking at 250 rpm in a 250-mL Erlenmeyer flask. Cells were harvested when the culture grew to OD_{600} 0.7 (in mid-log growth phase). Cells were washed twice with sterile phosphate-buffered saline (PBS) and then resuspended in PBS at a concentration of 2.0×10^6 colony-forming units (CFU)/mL. A Petroff-Hausser counting chamber was used to verify the concentration of the cell suspension and also confirmed by serial dilution and plating on LB agar using a spiral plating system (Autoplate®; Advanced Instruments, Inc., Norwood, MA).

Preparation of treatments

The neutropenic agent cyclophosphamide (Baxter, Deerfield, IL) was dissolved in 0.9% sodium chloride injection solution (Hospira, Inc., Lake Forest, IL) to obtain a final concentration of 100 mg/mL. Polymyxin B for topical application was compounded 0.1% in a 99:1 petrolatum to mineral oil base (Village Green Apothecary, Bethesda, MD).

Porcine dorsal wound model

A total of 13 female Yorkshire pigs weighing 30–35 kg were purchased from the Animal Biotech Industries (Doylestown, PA). All pigs received measured amounts of Laboratory Porcine Diet Grower 5084 (Purina LabDiet®, St. Louis, MO) and water *ad libitum*. All antibiotic administrations associated with husbandry were discontinued by the supplier >14 days before initiation of the procedures described below. Pigs were quarantined for >10 days in the Walter Reed Army Institute of Research (WRAIR) animal facility before initiation of the procedures described below. Pigs were housed singly in runs on elevated and rubberized cage grates. Pigs were treated humanely and in accordance with protocol 11-BRD-41L approved by the WRAIR/Naval Medical Research Center Institutional Animal Care and Use Committee (Silver Spring, MD). Five pigs were initially used in pilot studies to develop the model (data not shown). Three pigs ($n = 3$) were used to capture the neutrophil data presented in Fig. 2, and five pigs ($n = 5$) were used to collect the polymyxin-treated data compared to the untreated data that is presented.

Development of porcine wound infection model

Beginning on day 4 and at all subsequent time points, pigs were anesthetized with ketamine 12–20 mg/kg (Ketaset®; Fort Dodge Animal Health, Fort Dodge, IA) and xylazine 2.0–4.4 mg/kg (AnaSed®; Lloyd, Inc., Shenandoah, IA) intramuscular (IM) injection, followed by tracheal intubation and anesthetic maintenance on 2–4% isoflurane gas, and 1–3 mL intravenous (IV) blood sample was taken for complete blood count analyses. On day 4, each pig received 25 mg/kg cyclophosphamide via IV injection and was fitted with a customized canvas vest for acclimation before wounding and bandaging. On day 0, hair was clipped from the cervical to mid-lumbar dorsum, and the skin was scrubbed with iodine solution followed by a chlorhexidine rinse. A 12 mm (7 mm deep) disposable skin biopsy punch (Acuderm® Inc., Fort Lauderdale, FL) and surgical scissors were used to create 16 full-thickness skin defects into the subcutaneous fat overlying thoracic and lumbar paraspinal musculature. On day 0, 50 μL containing 5.0×10^4 AB5075 CFU in PBS suspension were pipetted into the wounds and allowed to absorb for 3 min. A transparent dressing (Tegaderm™ Film 1622 W; 3M Health Care, St. Paul, MN) was placed over each wound and secured with tissue adhesive (Vetbond™; 3M Animal Care, St. Paul, MN). A 75 mcg/h fentanyl patch (Duragesic®; Janssen Pharmaceuticals, Inc., Titusville, NJ) was placed on the pig flank and replaced at subsequent sampling time points. The pig torso was wrapped with bandaging tape (Vetrap™; 3M Animal Care), and the canvas vest was reapplied. Beginning on day 1 and at all subsequent time points, four

randomly assigned wound beds, one from each corner to account for anatomical variability, were sampled using a 4 mm disposable skin biopsy punch (Acuderm, Inc.). One of the wounds was cut into half. One half was collected for histopathology, as well as *A. baumannii* and wound healing marker–specific immunohistochemistry. The other half was collected for scanning electron microscopy (SEM). For the other biopsies collected on each day, four separate 4 mm punch biopsies within the 12 mm punch biopsy were used for analysis of CFU. Finally, wounds were closed with 3-0 polydioxanone suture material in an interrupted cruciate pattern (Fig. 1A–C).

Quantification of bacteria within the wound bed

Three replicate 4 mm biopsy punch tissue samples were evaluated per wound. Three wounds were evaluated per pig on days 2, 4, 7, and 10 postinocu-

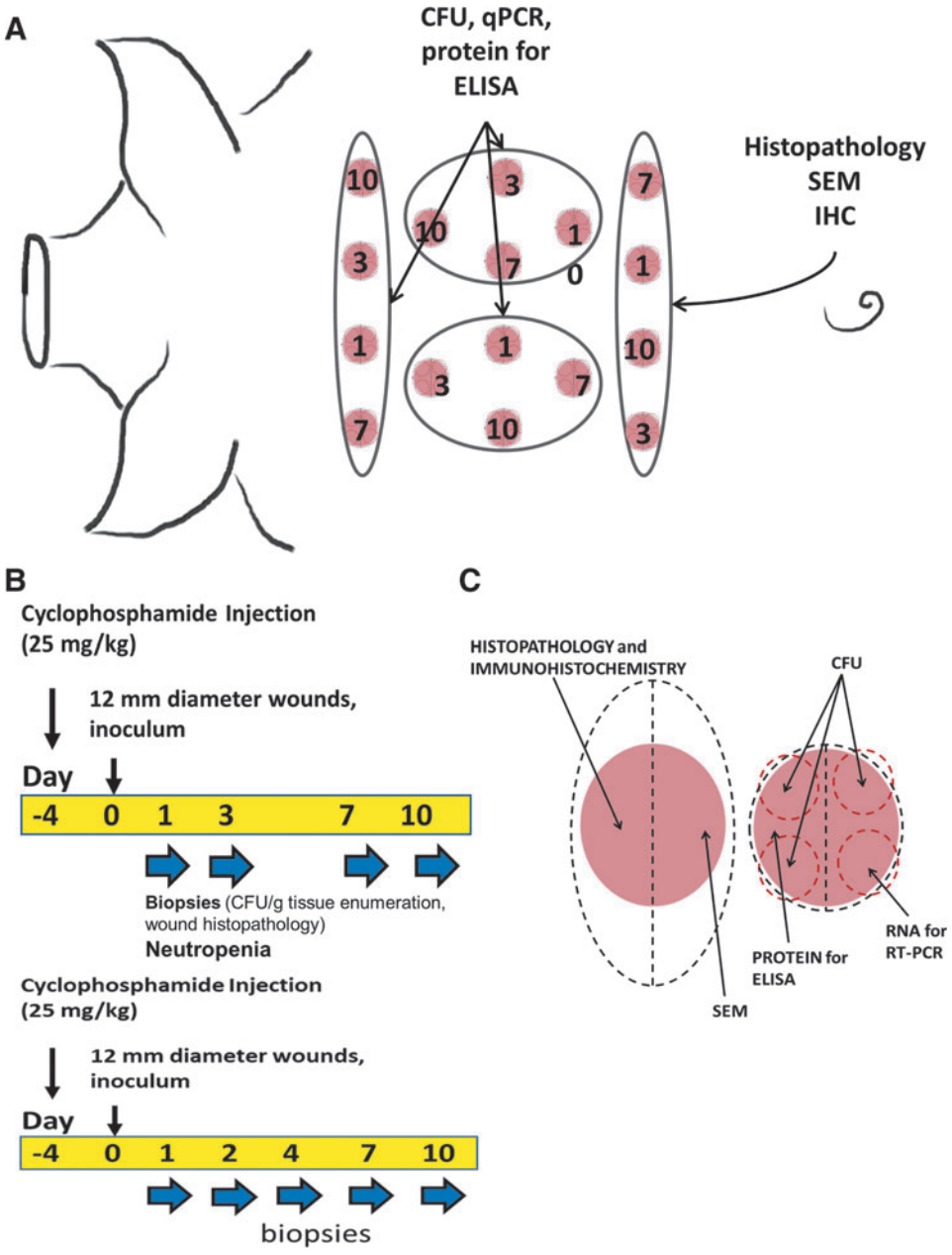

Figure 1. Animal model and experimental design. Porcine wound model cyclophosphamide and sampling regimen. The model uses Yorkshire pigs (female, 30–35 kg) that are given a single 25 mg/kg intravenous cyclophosphamide injection at day −4. **(A)** Representation of anatomical locations of the biopsies. **(B)** Timeline of experiment. Biopsies were collected on days 1, 3, 7, and 10. Since infection was found to be highest around day 3, we added another time point and collected samples on days 2 and 4 instead of day 3 in later experiments. **(C)** Sample site selection and postprocessing needs of skin biopsy sites. CFU, colony-forming units; SEM, scanning electron microscopy.

lation. The sample was placed in 1 mL of sterile PBS in a 14-mL conical tube and homogenized (TissueRuptor; Qiagen Sciences, Inc., Germantown, MD). Serial 10-fold dilutions of homogenate were plated via spiral plater onto eosin methylene blue agar (Becton, Dickinson and Co). Plates were incubated overnight at 37°C, and then, CFU were enumerated.

Quantitative and qualitative wound assessments

Wound area measurements were taken on the day of wounding and at subsequent time points using a Silhouette™ wound measurement device (Aranz Medical Limited, Christchurch, New Zealand). Time course wound photographs assessing gross pathology were taken using a Cannon digital single lens camera.

Scanning electron microscopy of wound bed and dressing

A single wound was evaluated per pig on days 2, 4, 7, and 10 postinoculation. The transparent dressings and a 4 mm biopsy punch tissue sample for each animal were fixed in 4% formaldehyde, 1% glutaraldehyde, and 0.1 M PBS. The samples were washed three times using 0.1 M PBS and then postfixed in 1% osmium tetroxide in 0.1 M PBS for 1 h. The samples were dehydrated in a graded series of ethanol solutions and then dried (Critical point dryer, Model 28000; Ladd Research Industries, Burlington, VT). The samples were mounted using a double-sided carbon tape to specimen stubs. They were then ion coated with gold:palladium (30:70) (Hummer X Sputter Coater; Anatech Ltd., Alexandria, VA). The samples were then visualized using an Amray 3600 FE scanning electron microscope (Bedford, MA) operated at a voltage of 3 kV and analyzed by scanning 10 or more 1,000× magnified fields within the wounded tissue and on the portion of the dressing overlying the wounded area. Photomicrographs representative of the observed bacterial density were taken at 2,500× magnification, which appears to be a biofilm.

Histological examinations of the wound bed

A single wound was evaluated per pig on days 2, 4, 7, and 10 postinoculation to characterize the histopathology of the model. The wounds were removed *en bloc* via elliptical excision. The tissue was halved; one portion was immediately fixed in phosphate-buffered formalin (10%) for >72 h, and the second portion was placed in 4% formalin at 4°C for subsequent immunohistochemistry. The wound tissue specimens were embedded in paraffin, cut in a dorsal–ventral plane bisecting the wound bed, and stained with hematoxylin–eosin (H&E) or peptide nucleic acid fluorescence *in situ* hybridization (PNA-FISH). Tissue was trimmed at 3 μm. For PNA-FISH, one drop of the PNA probe *Acinetobacter* PNA CP0050 (AdvanDx, Inc., Woburn, MA) was added to each slide, and coverslips were applied. Slides were put on a heating block for 90 min at 55°C in the dark. Slides were then immersed in preheated, 55°C deionized water for <1 min, while the coverslips (AdvanDx, Inc.) were removed. Slides were then immersed in preheated, 55°C 60× wash solution (AdvanDx, Inc.) for 30 min and then overlaid with coverslips by using the mounting medium (AdvanDx, Inc.).

Statistical analyses

All statistical analyses were carried out using GraphPad Prism software. Wound sizes, weight change, and CFU burdens were compared via the Kruskal–Wallis test, followed by Dunn's multiple comparison test. All results were considered significant if $p < 0.05$.

RESULTS

CFU burden in wound tissue

CFU/g was determined for each time point (days 3, 7, and 10). The wound bed and the dressing on top were assessed for CFU burden. As expected, CFU count was negligible for the uninfected pig for all wounds postinjury. For the infected pig, CFU burden was 1.0×10^7/g tissue by day 3 postinjury and gradually decreased on day 7 (although above clinically relevant infection level) and day 10. CFU burden demonstrated establishment of infection in the wounds (Fig. 2A).

Neutropenia associates with the CFU burden

Neutrophils are also measured at days –4, 0, 3, 7, and 10 and are represented by the blue (uninfected) and red lines (infected). Cyclophosphamide injection on day –4 successfully dropped the neutrophil count to zero by day 0. Neutrophil count was highly elevated following infection and stayed high above normal levels till the infection subsided (Fig. 2B).

Histopathological analysis of wound tissue demonstrates overt infection with the possibility of being a biofilm

SEM micrographs of Tegaderm dressing from the wound bed (day 3) were taken at 2,500× (Fig. 3A, C) and 5,000× (Fig. 3B, D) magnifications. Robust infection of AB5075 and extracellular polymeric substance suggests the development of a biofilm on the wound bed. An image at the wound edge demonstrates the presence of bacteria at the wound edge and the wound bed and not in the surrounding uninjured tissue (Fig. 3E).

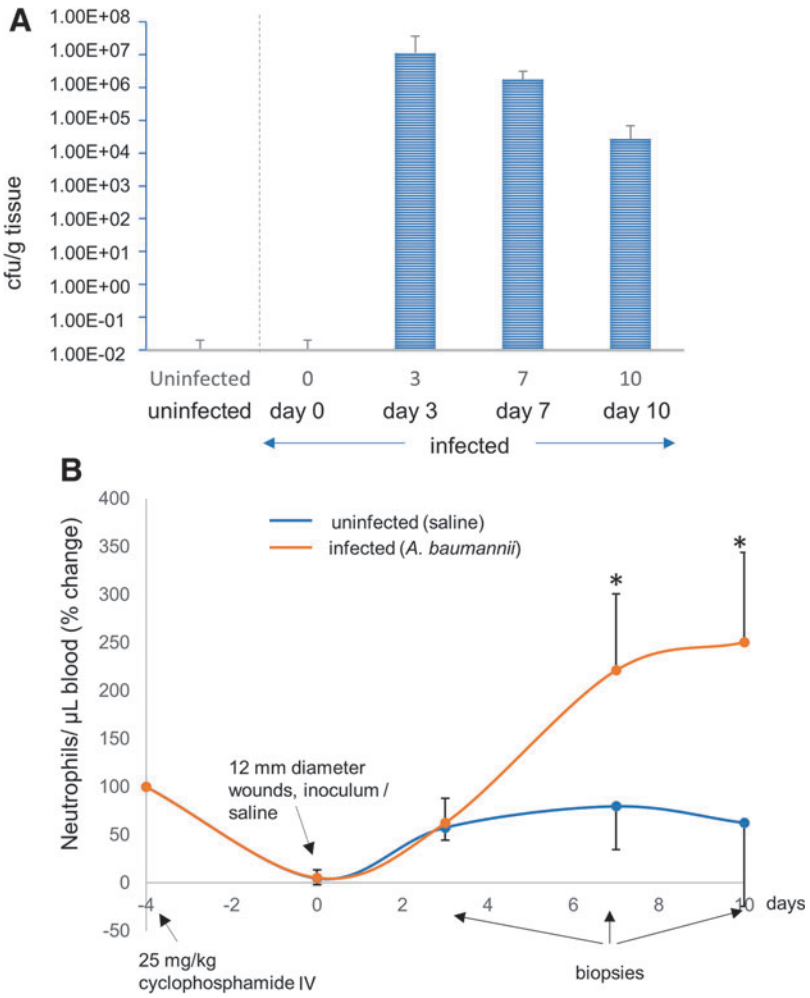

Figure 2. CFU and neutropenia. **(A)** CFU/g is determined for each time point, days 3, 7, and 10. **(B)** Neutrophils are also measured at days –4, 0, 3, 7, and 10 and are indicated by the *blue* and *red lines*, where *blue* represents the control pig that received no bacterial inoculum and *blue* represents the pigs inoculated with AB5075. *represents statistical significance when measured by Kruskal–Wallis test, followed by Dunn's multiple comparison test. IV, intravenous.

We also evaluated the infection status using PNA-FISH to understand where the bacteria were localized in animal tissue sections; because the highest infection was found to be around day 3, to get a better understanding of the infection timeline, we added another time point and collected samples on days 2 and 4 instead of day 3. Biopsies were evaluated at 20× and 60× using *Acinetobacter*-specific PNA probe–stained photomicrographs on days 2 and 7 to assess the bioburden. The green fluorescent probes demonstrate *A. baumannii* cells on day 2 (Fig. 4B–D). The reduction in green fluorescence on day 7 (Fig. 4E, F) demonstrates a clearance of *A. baumannii* cells after recruited neutrophils eradicate some of the bacterial burden. Regardless, some bacteria still coat the surface in a less robust infection. These observations correspond to the H&E staining, showing large colonization of bacteria on day 2 (Fig. 5A) and continued presence, although reduced on day 7 (Fig. 5B). For H&E staining, the low-magnification image shows the open wound area marked by arrows, while the zoomed-in image focuses on the bacteria. We also observed a lot of inflammatory cells, especially on days 2 and 4 when the bacterial load is highest, as corroborated from the CFU count. Dark edges indicate some necrotic tissue. By day 10, most of the wound has re-epithelialized. From the PNA-FISH images as well as from the H&E images, we observed that while at the surface the bacteria spread all across, deeper into the skin they appear in pockets (marked by arrows).

Susceptibility of the infection model to polymyxin B

We wanted to evaluate the effect of polymyxin B earlier in the infection because that is where the maximum colonization is observed, and so we added an additional biopsy time point (days 2 and 4) as opposed to one time point in day 3 in the

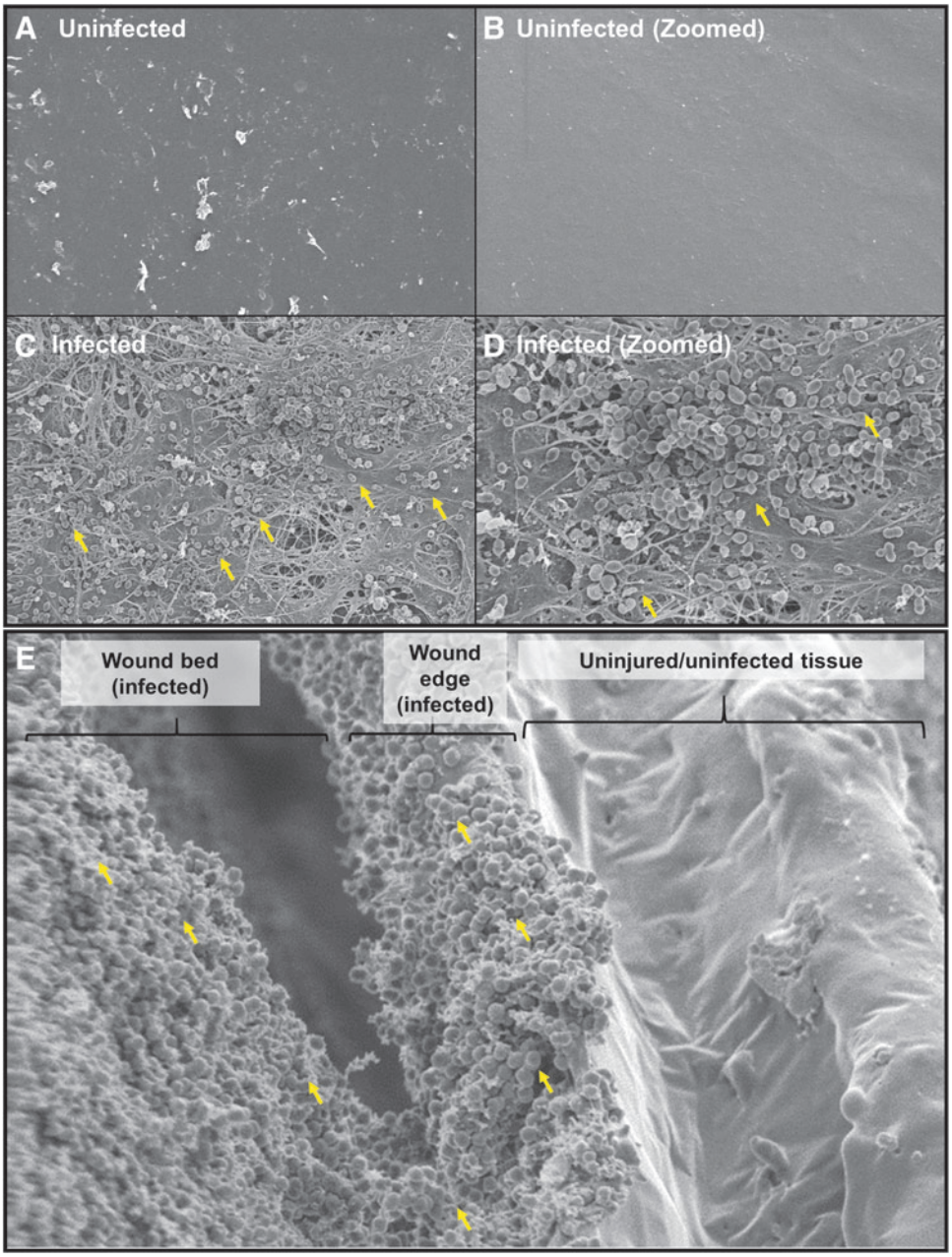

Figure 3. Scanning electron microscopy analysis of infection. SEM micrographs at **(A, C)** 2,500× and **(B, D)** 5,000× magnifications. As one can see, robust infection of AB5075 decorates the surface of the wound bed **(C, D)** and the clustered structure suggests a biofilm. Samples were from 4 mm punch biopsies taken at day 10. **(E)** SEM shows bacterial infection in the wound bed and the wound edge but absent at the surrounding uninjured tissue. *Yellow arrows* point to cocci in what appear to be biofilm.

previous experiment. Beginning on day 2 and at subsequent time points (days 4 and 7), pig wounds were treated with either 100 μL 0.1% polymyxin B topical ointment injected through the transparent dressing or the equivalent vehicle control (Fig. 6A).

We observed no difference in the CFU count on day 2 postinfection. However, from days 4 to 10 postinfection, the CFU/g tissue was found to be statistically significant (Fig. 6B). We also observed neutrophil counts from the blood on days 2, 4, 7, and 10. As the CFU count decreases, we found that the neutrophil count also decreased by day 7 in polymyxin B-treated pigs correlating with the decrease in the infection load (Fig. 6C).

DISCUSSION

The gram-negative *A. baumannii* has increasingly become a prevalent cause of hospital-acquired

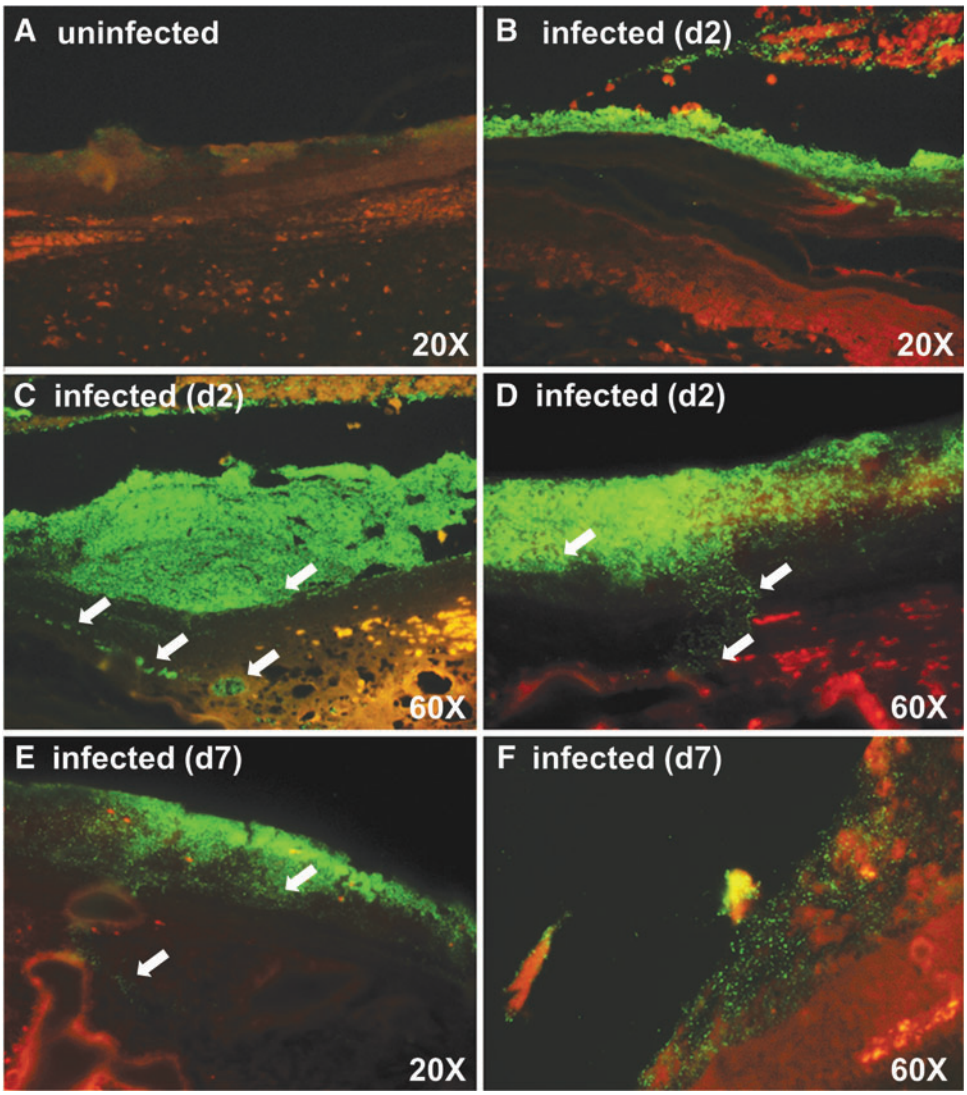

Figure 4. Peptide nucleic acid fluorescent *in situ* hybridization of pig wound biopsy. *Acinetobacter baumannii*-specific PNA probe (*fluorescent green*) labeled slides at days 2 and 7 (40× magnification). **(A)** An uninfected pig. **(B)** Day 2 and show a large infection. **(C, D)** Two separate zoomed-in regions of day 2 tissue. The *white arrows* point to bacteria that are deeper in the tissue, and these bacteria exist in what appear to be pockets. **(E)** Day 7 tissue and shows eradication of some of the bacterial burden after neutrophil recruitment. **(F)** Zoomed-in region of a day 7 tissue. Regardless, some bacteria still coat the surface in a less robust infection.

infections during the last two decades. *A. baumannii* is now responsible for >10% of all hospital-acquired infections in the United States and has a >50% mortality rate in patients with sepsis and pneumonia. Due to their resistance to the first-line agents, XDR *A. baumannii* bloodstream infections result in >50–60% mortality (up to 70% mortality rate from infections caused by XDR strains in some case series).[8,28,29] Traumatic injury or surgery patients often require extensive hospitalization during recovery, increasing the risk for wound and surgical site infections caused by ESKAPE pathogens, such as *A. baumannii*.[17] Further complicating treatment options is the increase in MDR and XDR strains of *A. baumannii*.[30] Thus, new drugs being developed with a sharper focus on *Acinetobacter* species and are urgently in need of evaluation[2,31,32] before entry into clinical trials.

To test novel drugs specifically targeting *A. baumannii* infection, it is essential to test the drugs in clinically relevant animal models to validate *in vitro* results.[33] The development of an animal model for *A. baumannii* infection can be difficult to implement because the majority of clinical *A. baumannii* isolates display high-level resistance to antimicrobials and most strains are not terribly virulent. Additionally, host neutrophils directly contribute toward host resistance of cutaneous

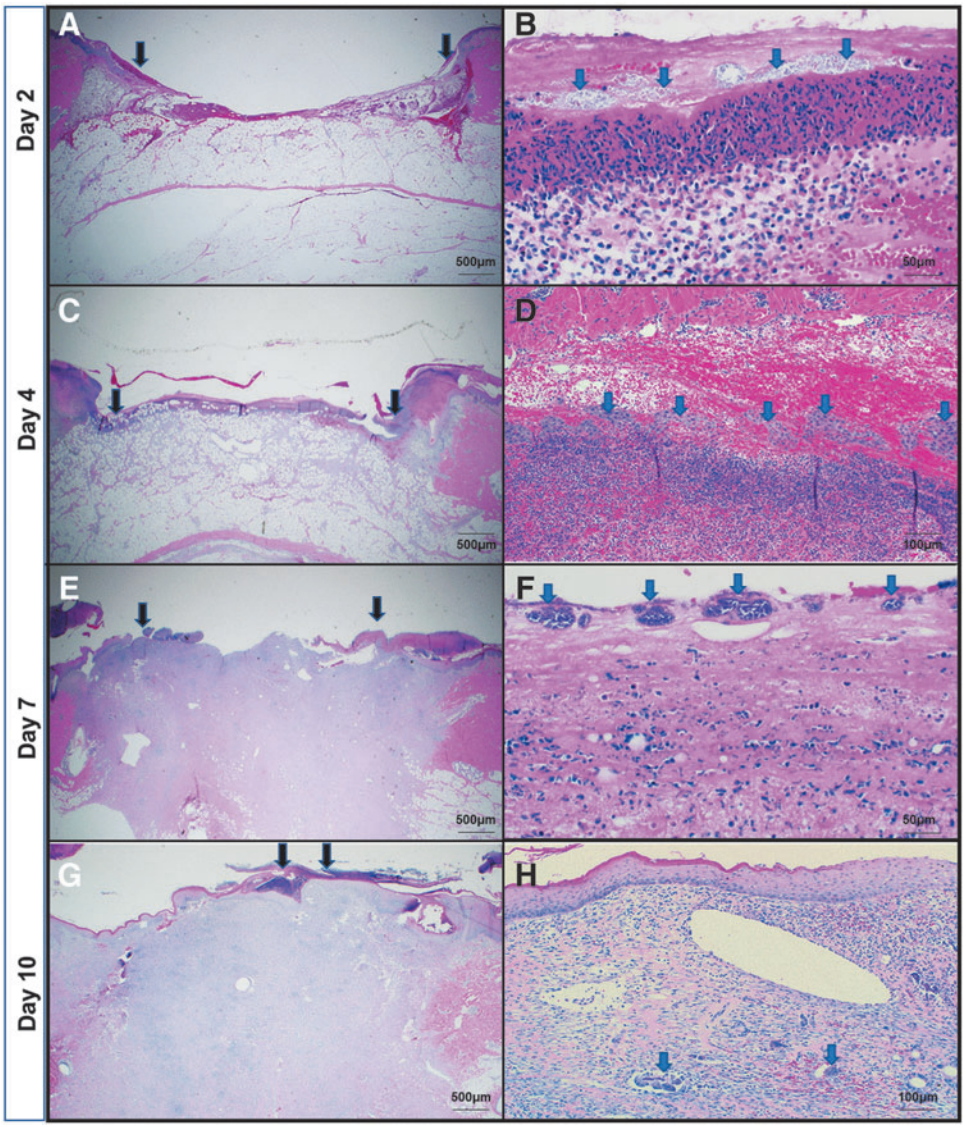

Figure 5. Hematoxylin–eosin staining of pig wound biopsy. **(A, C, E, G)** reveals the open wound area (the edges marked by *black arrows*). **(B, D, F, H)** focuses on the presence of bacterial colonies (stained as *grey dots*, marked with *blue arrows*).

A. baumannii infection. Clinical studies have shown that *A. baumannii* is one of the most frequently isolated gram-negative bacteria in neutropenic febrile patients in nosocomial settings,[34–38] particularly after prolonged hospitalization.[39] Cyclophosphamide suppresses myelopoiesis resulting in neutrophil depletion in murine models,[40] and to develop a sustained infection model, cyclophosphamide has been widely used.[17,40–44] Other neutropenic models used Ly-6G-specific monoclonal antibody 1A8,[41] mucin,[42] or morphine[43] to establish neutropenia and study the pathogenesis of several *A. baumannii* clinical isolates on wounded cutaneous tissue. Intravenous inoculums have also been used to induce sepsis and evaluate treatments in murine models[44–46] and yet another model used diabetic mice.[47] Some groups have successfully developed reproducible *A. baumannii* infections using more virulent isolates in immunocompetent and conventional mouse strains.[48–50] However, these more virulent isolates have a different capsule and represent only 5% of all the strains the military has collected so the occurrence in the clinic appears to be a rare event.[49] In contrast, AB5075 is an ST2 strain, which is the most isolated ST group with regard to outbreaks,[51] and most clinical isolates are less virulent and require neutropenia for a successful infection in most animal models. It should also be noted that the route of administration and animal strain selection

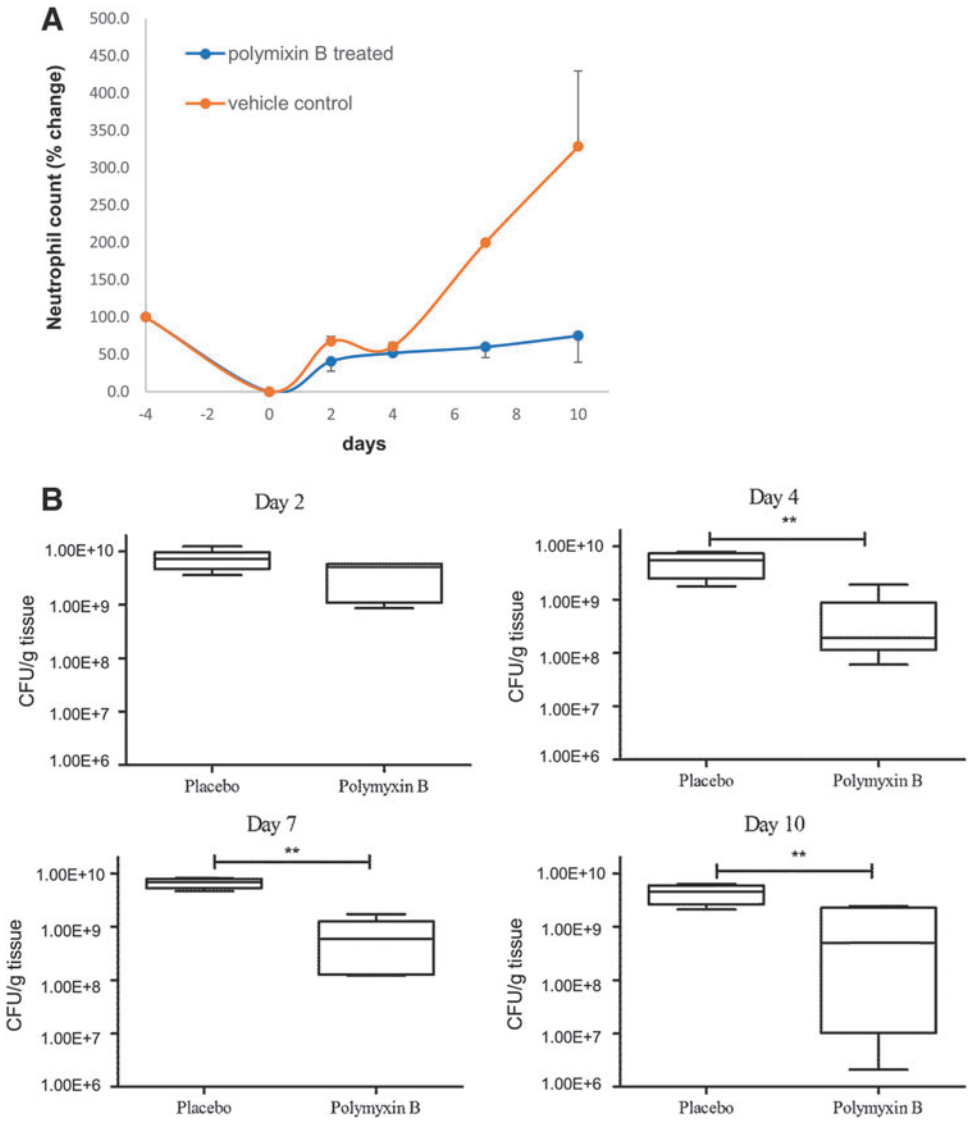

Figure 6. Neutrophil count and CFU/g tissue in polymyxin B-treated versus untreated pigs. **(A)** Neutrophil count correlated with bacterial load and was found to decrease after treatment with polymyxin B. **(B)** The CFU count remains unchanged on day 2 postinfection (p.i.) between placebo-treated and polymyxin B-treated samples. From days 4 to 10 p.i., the CFU/g tissue was significantly lower in polymyxin-B treated samples. **repesents statistical significance when measured by Kruskal–Wallis test, followed by Dunn's multiple comparison test.

matter as AB5075 in a pulmonary model did lead to animal death in C57/Bl6 mice,[52] while we did not observe this with Balb/C mice[14] using the same inoculating dose of bacteria.

With regard to the porcine model, our pilot experiments failed to establish a successful and sustained infection with *A. baumannii*, without relying on a temporary neutropenia. The final dose of cyclophosphamide that was described in the Materials and Methods section is quite low, but optimized and sufficient to induce an infection. Unfortunately, a higher inoculum of *A. baumannii* into the wound bed without neutropenia resulted in animal mortality likely due to sepsis. In contrast, when a larger dose of cyclophosphamide was used, we observed a similar result with just 10^4 CFU inoculum, mortality likely due to dissemination and sepsis. So the model relies on a balance of inoculum and cyclophosphamide to find a "sweet spot" where animals do not perish, but we still see a lasting infection in the wound bed. A caveat with respect to all models is that these results may not accurately reproduce some features of infection and wound healing in non-neutropenic patients, as neutrophils play an important role in the early stages of healing. However, nonhealing wounds, specially diabetic and aging wounds are often associated with reduced neutrophil infiltration,[53–56]

and therefore, a neutropenic model can still be an useful tool and a good representation to study *A. baumannii* infection and to test novel antibiotics designed to reduce bacterial load.

While many animal models that study wound infection are often thermal injury models,[57–59] our laboratory developed a murine cutaneous excision wound model in which antimicrobials could be evaluated from multiple quantitative/qualitative and microbiological/wound healing endpoints throughout a longer duration aggressive *A. baumannii* infection.[17] None of the aforementioned models, however, developed something similar with a large animal and an indication for SSTI. A porcine model is useful for wound healing studies as the pig skin is a good approximation of the human skin and resembles most closely that of humans structurally and physiologically.[21] Both pigs and humans have a thick epidermis and a similar dermal:epidermal thickness ratio. Well-developed rete-ridges, dermal papillary bodies, subdermal adipose tissue, dermal collagen content, size, orientation, distribution of blood vessels in the dermis of the pigs and humans, adnexal structures, and hair are comparable between human and porcine skin. An additional important reason for considering the pig as a better model for wound healing studies is because humans and pigs heal through physiologically similar processes. Most rodents and small animals have a panniculus carnosus and rely on wound contraction for wound closure. Humans and pigs, however, do not have the panniculus carnosus and close partial-thickness wounds largely through re-epithelialization.[21] Development of a porcine infection model is therefore the next logical step after we established our murine *A. baumannii* infection model.

To reiterate, establishing the porcine model required two steps: a pretreatment to limit the immune response and an inoculation that led to an infection. Infection could be defined by various measures to include CFU reaching a level beyond 1.0×10^7, which is where we have seen pus, necrotic tissue, swelling, and other indicators of infection in our murine model of *A. baumannii* infection[17] and consistent with what is seen in human patients.[60] In order for the infection to progress and reach these endpoints with a relatively small inoculum, the pigs needed to be slightly immunosuppressed. In this case, we followed guidance from a previous work that utilized cyclophosphamide to establish a *Haemophilus ducreyi* infection in Yorkshire pigs.[61] In that model, they used 50 mg/kg for 4 days pre-inoculation and 20 mg/kg every other day until inoculation and biopsies were taken, out to day 7.[61] To start, we decided on 50 mg/kg cyclophosphamide on day 4 (4 days pre-inoculum) and 25 mg/kg on Day 2. Then, pigs were wounded and inoculated, but one animal subsequently perished from what we believe (necropsy nonconclusive) was sepsis a few days after inoculation. Therefore, the cyclophosphamide dosage was dialed back to just one pretreatment of cyclophosphamide at a dosage of 25 mg/kg (see the Results section). At this concentration, we still observed increases in *A. baumannii* CFU, but death was not observed in any animal for the duration of the experiment. This was similar to what we achieved in our mouse model of infection,[17] and that similarity between the models allowed us to speculate that the pathogenesis of the bacteria in both animals could be the same.

Most research on the pathogenicity of *A. baumannii* focused on isolates that are not truly representative of current MDR strains isolated from patients. After screening of a panel of isolates in different *in vitro* and *in vivo* assays, AB5075 was selected as a model strain more suitable for research because of its antibiotic resistance profile and increased virulence in three different animal models.[14] We note, however, that while cyclophosphamide is a valuable tool to limit neutrophils and understand some aspects of pathogenesis, it also depletes suppressor or regulatory T cells[62,63] and affects circulating macrophages.[64] Therefore, a limitation of this model would be understanding the impact of these immune cells with regard to *A. baumannii* infection. Therefore, use of something that preferentially works on neutrophils, such as mAb1A8 that was used in mice[34] may be a way to further improve this porcine model. However, given the size difference, it would be an expensive experiment. That said, the model still allows for the evaluation of some aspects of *A. baumannii* pathogenesis as the bacteria attached and colonized the wound bed, established an infection, and what appears to be a biofilm is formed in the wound bed subsequent days after the initial inoculum and concordant with the destruction of tissue. So, while there is limitation with regard to the immune response, the model is still valuable for antibiotic testing and studying pathogenesis.

In conclusion, we present here an excisional porcine wound model in which a diminutive inoculum of a clinically relevant XDR *A. baumannii* isolate that can proliferate, infect, and possibly form biofilms, and be effectively treated with antibiotics. Colistin (polymyxin E) and polymyxin B are the two clinically used forms polymyxins, which are widely

used,[65] and polymyxin B was effective in reducing bacterial load against AB5075, a polymyxin-susceptible strain, used in this work. However, the use of polymyxins is limited by their nephrotoxic and neurotoxic effects and hence administered mostly to prevent rather than treat infections.[66,67] In addition, there has been a surge in reports of infections caused by naturally occurring polymyxin-resistant bacteria so novel approaches to eradicate *A. baumannii* infection are still needed. We note that although polymyxin was found to have a significant effect on bacterial load, the bacterial numbers still hold higher than what would be considered a clinical threshold for wound infection, $>10^5$–10^6 CFU. However, to be clear, this set of experiments was more to establish the infection with AB5075 and just validate the susceptibility of this strain to polymyxin in the model. These experiments were not intended to test the efficacy of polymyxin treatment. In the future, to establish polymyxin B as a positive control in this model, an increase in the dosage or the number of doses provided would be required. Nonetheless, there is an urgency to test new topical drugs against MDR and XDR *Acinetobacter*, and our preclinical model can be a valuable platform to evaluate the efficacy of such drugs in infected wounds. While we note that biological membranes, over time, develop mixed species infection due to the normal flora of the skin itself, every attempt should be made to narrow the antibiotic spectrum as it can reduce cost and toxicity and prevent the emergence of antimicrobial resistance in the community.[68] A single species–infected model like the one that we present here can serve this purpose to test narrow-spectrum antibiotics against *A. baumannii.*

INNOVATION

Drug-resistant wound infections are occurring with more regularity, and novel treatments are needed. Specifically, *A. baumannii* is often linked to MDR infections, where the first, and often the second choice of antibiotic, results in treatment failure. With the introduction of AB5075 in a preclinical porcine excision model, we have successfully simulated an *A. baumannii* SSTI wound infection in a large animal model that can be used preclinically to test new antibacterials. This is a significant innovation as previous porcine models that utilized *A. baumannii* were polymicrobial with more than one infectious agent. As numerous pharmaceutical companies and academic laboratories drive to develop narrow-spectrum *A. baumannii*-specific therapies, single agent models where *A. baumannii* is the sole infectious agent are needed for preclinical testing.

ACKNOWLEDGMENTS AND FUNDING SOURCES

We thank Dr. Xiaorong Feng, Dr. Crystal Jones, and others in the Wound Infections Department (WID) at the WRAIR for their technical support; these studies would not be possible without them. The research presented was funded by the Military Infectious Diseases Research Program. Material has been reviewed by the WRAIR. There is no objection to its presentation and/or publication. The opinions or assertions contained herein are the private views of the authors and are not to be construed as official or as reflecting true views of the Department of the Army or the Department of Defense. Research was conducted under an approved animal protocol (11-BRD-41L) in an AAALACi-accredited facility in compliance with the Animal Welfare Act and other federal statutes and regulations relating to animals and experiments involving animals and adheres to principles stated in the Guide for the Care and Use of Laboratory Animals, NRC Publication, 2011 edition.

AUTHOR DISCLOSURE AND GHOSTWRITING STATEMENT

No competing financial interests exist. The content of this article was expressly written by the authors listed. No ghostwriters were used to write this article.

ABOUT THE AUTHORS

Daniel V. Zurawski, PhD, has been a principal investigator (PI) at the WRAIR in the Bacterial Diseases Branch (BDB), WID for 9 years. He and his team utilize novel microbiology approaches and animal modeling to design and test novel antibacterial strategies against MDR-ESKAPE pathogens. In addition, Dr. Zurawski has numerous collaborations with industry and academic partners. **LTC Chad C. Black, DVM, PhD,** is the Deputy Director of the Experimental Therapeutics Branch at WRAIR where he oversees operations for the U.S. Army's small molecule pharmaceutical incubator tasked with developing the next generation of malaria chemoprophylaxis and antibiotics for resistant infections. Previously, he was Chief of Animal Support in WID. **Yonas A. Alamneh, MS,** is manager of Animal Support in WID. **Lionel Biggemann, MS,** was a technician in WID. **Jaideep Banerjee, PhD,** is a technical writer for WID. **Mitchell G. Thompson, BA,** was a technician in WID. **Matthew C. Wise, BS,** is a staff member of the Department of Pathology. **LTC Cary L. Honnold, DVM, DACVP,** was the previous Chief of the Department of Pathology at

WRAIR. **MAJ Robert K. Kim, DVM, PhD,** was previous Chief of Animal Support in WID. **Chrysanthi Paranavitana, PhD,** was a previous PI in WID. **Jonathan P. Shearer, PhD,** is the Current Chief of Animal Support in the WID. **Stuart D. Tyner, PhD,** is the Director of the BDB and previous Chief of WID. **Samandra T. Demons, PhD,** is the Current Chief of WID.

KEY FINDINGS

- Both academia and the pharmaceutical industry are developing narrow-spectrum antibacterials for *A. baumannii*, and this is the first porcine model where *A. baumannii* is used as the sole infectious agent.
- The infection progresses for 7 days, and the bacteria possibly form a biofilm both in the wound bed and on the overlying dressing.
- A topical antibiotic, polymyxin B, could be applied, and bacterial burden in the wound was significantly reduced.

REFERENCES

1. Zapor MJ, Moran KA. Infectious diseases during wartime. Curr Opin Infect Dis 2005;18:395–399.
2. Howard A, O'Donoghue M, Feeney A, Sleator RD. *Acinetobacter baumannii*: an emerging opportunistic pathogen. Virulence 2012;3:243–250.
3. Villegas MV, Hartstein AI. Acinetobacter outbreaks, 1977–2000. Infect Control Hosp Epidemiol 2003;24:284–295.
4. Scott P, Deye G, Srinivasan A, et al. An outbreak of multidrug-resistant *Acinetobacter baumannii-calcoaceticus* complex infection in the US military health care system associated with military operations in Iraq. Clin Infect Dis 2007;44:1577–1584.
5. Sebeny PJ, Riddle MS, Petersen K. *Acinetobacter baumannii* skin and soft-tissue infection associated with war trauma. Clin Infect Dis 2008;47: 444–449.
6. Hujer KM, Hujer AM, Hulten EA, et al. Analysis of antibiotic resistance genes in multidrug-resistant Acinetobacter sp. isolates from military and civilian patients treated at the Walter Reed Army Medical Center. Antimicrob Agents Chemother 2006;50:4114–4123.
7. Yun HC, Branstetter JG, Murray CK. Osteomyelitis in military personnel wounded in Iraq and Afghanistan. J Trauma 2008;64(2 Suppl):S163–S168; discussion S168.
8. Wong D, Nielsen TB, Bonomo RA, Pantapalangkoor P, Luna B, Spellberg B. Clinical and Pathophysiological Overview of Acinetobacter Infections: a Century of Challenges. Clin Microbiol Rev 2017;30:409–447.
9. Grosso F, Quinteira S, Peixe L. Emergence of an extreme-drug-resistant (XDR) *Acinetobacter baumannii* carrying blaOXA-23 in a patient with acute necrohaemorrhagic pancreatitis. J Hosp Infect 2010;75:82–83.
10. Moffatt JH, Harper M, Harrison P, et al. Colistin resistance in *Acinetobacter baumannii* is mediated by complete loss of lipopolysaccharide production. Antimicrob Agents Chemother 2010;54:4971–4977.
11. Dafopoulou K, Xavier BB, Hotterbeekx A, et al. Colistin-resistant *Acinetobacter baumannii* clinical strains with deficient biofilm formation. Antimicrob Agents Chemother 2015;60:1892–1895.
12. Qureshi ZA, Hittle LE, O'Hara JA, et al. Colistin-resistant *Acinetobacter baumannii*: beyond carbapenem resistance. Clin Infect Dis 2015;60:1295–1303.
13. Pelletier MR, Casella LG, Jones JW, et al. Unique structural modifications are present in the lipopolysaccharide from colistin-resistant strains of *Acinetobacter baumannii*. Antimicrob Agents Chemother 2013;57:4831–4840.
14. Jacobs AC, Thompson MG, Black CC, et al. AB5075, a highly virulent isolate of *Acinetobacter baumannii*, as a model strain for the evaluation of pathogenesis and antimicrobial treatments. mBio 2014;5:e01076–01014.
15. Russo TA, Beanan JM, Olson R, et al. Rat pneumonia and soft-tissue infection models for the study of *Acinetobacter baumannii* biology. Infect Immun 2008;76:3577–3586.
16. Chen L, Mirza R, Kwon Y, DiPietro LA, Koh TJ. The murine excisional wound model: contraction revisited. Wound Repair Regen 2015;23:874–877.
17. Thompson MG, Black CC, Pavlicek RL, et al. Validation of a novel murine wound model of *Acinetobacter baumannii* infection. Antimicrob Agents Chemother 2014;58:1332–1342.
18. Thompson MG, Truong-Le V, Alamneh YA, et al. Evaluation of Gallium Citrate Formulations against a Multidrug-Resistant Strain of *Klebsiella pneumoniae* in a Murine Wound Model of Infection. Antimicrob Agents Chemother 2015;59:6484–6493.
19. Regeimbal JM, Jacobs AC, Corey BW, et al. Personalized therapeutic cocktail of wild environmental phages rescues mice from *Acinetobacter baumannii* wound infections. Antimicrob Agents Chemother 2016;60:5806–5816.
20. Greenhalgh DG. Models of wound healing. J Burn Care Rehabil 2005;26:293–305.
21. Sullivan TP, Eaglstein WH, Davis SC, Mertz P. The pig as a model for human wound healing. Wound Repair Regen 2001;9:66–76.
22. Abouelhassan Y, Yang Q, Yousaf H, et al. Nitroxoline: a broad-spectrum biofilm-eradicating agent against pathogenic bacteria. Int J Antimicrob Agents 2017;49:247–251.
23. Richmond GE, Evans LP, Anderson MJ, et al. The *Acinetobacter baumannii* two-component system aders regulates genes required for multidrug efflux, biofilm formation, and virulence in a strain-specific manner. mBio 2016;7:e00430–00416.
24. Roy S, Elgharably H, Sinha M, et al. Mixed-species biofilm compromises wound healing by disrupting epidermal barrier function. J Pathol 2014;233:331–343.
25. Mendes JJ, Leandro C, Corte-Real S, et al. Wound healing potential of topical bacteriophage therapy on diabetic cutaneous wounds. Wound Repair Regen 2013;21:595–603.
26. Be NA, Allen JE, Brown TS, et al. Microbial profiling of combat wound infection through detection microarray and next-generation sequencing. J Clin Microbiol 2014;52:2583–2594.
27. Zurawski DV, Thompson MG, McQueary CN, et al. Genome sequences of four divergent multidrug-resistant *Acinetobacter baumannii* strains isolated from patients with sepsis or osteomyelitis. J Bacteriol 2012;1941619–1620.
28. Spellberg B, Rex JH. The value of single-pathogen antibacterial agents. Nat Rev Drug Discov 2013; 12:963.
29. Esterly JS, Griffith M, Qi C, Malczynski M, Postelnick MJ, Scheetz MH. Impact of carbapenem resistance and receipt of active antimicrobial therapy on clinical outcomes of *Acinetobacter baumannii* bloodstream infections. Antimicrob Agents Chemother 2011;55:4844–4849.
30. Chung JH, Bhat A, Kim CJ, Yong D, Ryu CM. Combination therapy with polymyxin B and netropsin against clinical isolates of multidrug-resistant *Acinetobacter baumannii*. Sci Rep 2016;6:28168.
31. Johnson EN, Burns TC, Hayda RA, Hospenthal DR, Murray CK. Infectious complications of open type III tibial fractures among combat casualties. Clin Infect Dis 2007;45:409–415.
32. Mihu MR, Martinez LR. Novel therapies for treatment of multi-drug resistant *Acinetobacter baumannii* skin infections. Virulence 2011;2:97–102.

33. Marra A. A review of animal models used for antibiotic evaluation. In: Dougherty T, Pucci M, eds. Antibiotic Discovery and Development. Boston, MA: Springer, 2012.

34. Karim M, Khan W, Farooqi B, Malik I. Bacterial isolates in neutropenic febrile patients. J Pak Med Assoc 1991;41:35–37.

35. Fukuta Y, Muder RR, Agha ME, et al. Risk factors for acquisition of multidrug-resistant *Acinetobacter baumannii* among cancer patients. Am J Infect Control 2013;41:1249–1252.

36. Yadegarynia D, Fatemi A, Mahdizadeh M, Kabiri Movahhed R, Alizadeh MA. Current spectrum of bacterial infections in patients with nosocomial fever and neutropenia. Caspian J Intern Med 2013;4698–701.

37. Kim Y, Bae IK, Lee H, Jeong SH, Yong D, Lee K. In vivo emergence of colistin resistance in *Acinetobacter baumannii* clinical isolates of sequence type 357 during colistin treatment. Diagn Microbiol Infect Dis 2014;79362–366.

38. Kim SB, Min YH, Cheong JW, et al. Incidence and risk factors for carbapenem- and multidrug-resistant *Acinetobacter baumannii* bacteremia in hematopoietic stem cell transplantation recipients. Scand J Infect Dis 2014;46:81–88.

39. Higgins PG, Wisplinghoff H, Stefanik D, Seifert H. In vitro activities of the beta-lactamase inhibitors clavulanic acid, sulbactam, and tazobactam alone or in combination with beta-lactams against epidemiologically characterized multidrug-resistant *Acinetobacter baumannii* strains. Antimicrob Agents Chemother 2004;481586–1592.

40. Zuluaga AF, Salazar BE, Rodriguez CA, Zapata AX, Agudelo M, Vesga O. Neutropenia induced in outbred mice by a simplified low-dose cyclophosphamide regimen: characterization and applicability to diverse experimental models of infectious diseases. BMC Infect Dis 2006;6:55.

41. Grguric-Smith LM, Lee HH, Gandhi JA, et al. Neutropenia exacerbates infection by *Acinetobacter baumannii* clinical isolates in a murine wound model. Front Microbiol 2015;6:1134.

42. Montero A, Ariza J, Corbella X, et al. Efficacy of colistin versus beta-lactams, aminoglycosides, and rifampin as monotherapy in a mouse model of pneumonia caused by multiresistant *Acinetobacter baumannii*. Antimicrob Agents Chemother 2002;46:1946–1952.

43. Breslow JM, Monroy MA, Daly JM, et al. Morphine, but not trauma, sensitizes to systemic *Acinetobacter baumannii* infection. J Neuroimmune Pharmacol 2011;6:551–565.

44. Gaddy JA, Arivett BA, McConnell MJ, Lopez-Rojas R, Pachon J, Actis LA. Role of acinetobactin-mediated iron acquisition functions in the interaction of *Acinetobacter baumannii* strain ATCC 19606T with human lung epithelial cells, Galleria mellonella caterpillars, and mice. Infect Immun 2012;80:1015–1024.

45. Cirioni O, Silvestri C, Ghiselli R, et al. Therapeutic efficacy of buforin II and rifampin in a rat model of *Acinetobacter baumannii* sepsis. Crit Care Med 2009;37:1403–1407.

46. Shankar R, He LK, Szilagyi A, et al. A novel antibacterial gene transfer treatment for multidrug-resistant *Acinetobacter baumannii*-induced burn sepsis. J Burn Care Res 2007;28:6–12.

47. Luo G, Spellberg B, Gebremariam T, et al. Diabetic murine models for *Acinetobacter baumannii* infection. J Antimicrob Chemother 2012;67:1439–1445.

48. Harris G, Kuo Lee R, Lam CK, et al. A mouse model of *Acinetobacter baumannii*-associated pneumonia using a clinically isolated hypervirulent strain. Antimicrob Agents Chemother 2013;57:3601–3613.

49. Jones CL, Clancy M, Honnold C, et al. Fatal outbreak of an emerging clone of extensively drug-resistant *Acinetobacter baumannii* with enhanced virulence. Clin Infect Dis 2015;61:145–154.

50. Bruhn KW, Pantapalangkoor P, Nielsen T, et al. Host fate is rapidly determined by innate effector-microbial interactions during *Acinetobacter baumannii* bacteremia. J Infect Dis 2015;211:1296–1305.

51. Wallace L, Daugherty SC, Nagaraj S, Johnson JK, Harris AD, Rasko DA. Use of comparative genomics to characterize the diversity of *Acinetobacter baumannii* surveillance isolates in a health care institution. Antimicrob Agents Chemother 2016;60:5933–5941.

52. Chin CY, Tipton KA, Farokhyfar M, Burd EM, Weiss DS, Rather PN. A high-frequency phenotypic switch links bacterial virulence and environmental survival in *Acinetobacter baumannii*. Nat Microbiol 2018;3:563–569.

53. Manepalli S, Gandhi JA, Ekhar VV, Asplund MB, Coelho C, Martinez LR. Characterization of a cyclophosphamide-induced murine model of immunosuppression to study *Acinetobacter baumannii* pathogenesis. J Med Microbiol 2013;62(Pt 11):1747–1754.

54. Ebaid H. Neutrophil depletion in the early inflammatory phase delayed cutaneous wound healing in older rats: improvements due to the use of un-denatured camel whey protein. Diagn Pathol 2014;9:46.

55. Brubaker AL, Rendon JL, Ramirez L, Choudhry MA, Kovacs EJ. Reduced neutrophil chemotaxis and infiltration contributes to delayed resolution of cutaneous wound infection with advanced age. J Immunol 2013;190:1746–1757.

56. Su Y, Richmond A. Chemokine Regulation of Neutrophil Infiltration of Skin Wounds. Adv Wound Care (New Rochelle) 2015;4:631–640.

57. Mihu MR, Sandkovsky U, Han G, Friedman JM, Nosanchuk JD, Martinez LR. The use of nitric oxide releasing nanoparticles as a treatment against *Acinetobacter baumannii* in wound infections. Virulence 2010;1:62–67.

58. Dai T, Huang YY, Hamblin MR. Photodynamic therapy for localized infections—state of the art. Photodiagnosis Photodyn Ther 2009;6:170–188.

59. DeLeon K, Balldin F, Watters C, et al. Gallium maltolate treatment eradicates *Pseudomonas aeruginosa* infection in thermally injured mice. Antimicrob Agents Chemother 2009;53:1331–1337.

60. Bendy RH, Jr., Nuccio PA, Wolfe E, et al. Relationship of Quantitative Wound Bacterial Counts to Healing of Decubiti: effect of Topical Gentamicin. Antimicrob Agents Chemother (Bethesda) 1964;10:147–155.

61. Fernandez de la Hoz K, de Mateo S, Regidor E. [Trends in infectious diseases mortality in Spain]. Gac Sanit 1999;13:256–262.

62. Yasunami R, Bach JF. Anti-suppressor effect of cyclophosphamide on the development of spontaneous diabetes in NOD mice. Eur J Immunol 1988;18:481–484.

63. Ghiringhelli F, Larmonier N, Schmitt E, et al. CD4+CD25+ regulatory T cells suppress tumor immunity but are sensitive to cyclophosphamide which allows immunotherapy of established tumors to be curative. Eur J Immunol 2004;34:336–344.

64. Santosuosso M, Divangahi M, Zganiacz A, Xing Z. Reduced tissue macrophage population in the lung by anticancer agent cyclophosphamide: restoration by local granulocyte macrophage-colony-stimulating factor gene transfer. Blood 2002;99:1246–1252.

65. Shaheen M, Li J, Ross AC, Vederas JC, Jensen SE. Paenibacillus polymyxa PKB1 produces variants of polymyxin B-type antibiotics. Chem Biol 2011;18:1640–1648.

66. Huttner B, Jones M, Rubin MA, Neuhauser MM, Gundlapalli A, Samore M. Drugs of last resort? The use of polymyxins and tigecycline at US Veterans Affairs medical centers, 2005–2010. PLoS One 2012;7:e36649.

67. Falagas ME, Kasiakou SK. Toxicity of polymyxins: a systematic review of the evidence from old and recent studies. Crit Care 2006;10:R27.

68. Leekha S, Terrell CL, Edson RS. General principles of antimicrobial therapy. Mayo Clin Proc 2011;86:156–167.

Abbreviations and Acronyms

ABSSSI = acute bacterial skin and skin structure infections
CFU = colony-forming units
ESKAPE pathogens = *Enterococcus faecium*, *Staphylococcus aureus*, *Klebsiella pneumoniae*, *Acinetobacter baumannii*, *Pseudomonas aeruginosa*, and *Enterobacter* species.
H&E = hematoxylin–eosin
IV = intravenous
LB = Luria–Bertani
MDR = multidrug-resistant
PBS = phosphate-buffered saline
PNA-FISH = peptide nucleic acid fluorescence *in situ* hybridization
SEM = scanning electron microscopy
SSTI = skin and soft tissue infections
WID = Wound Infections Department
WRAIR = Walter Reed Army Institute of Research
XDR = extensively drug-resistant